

## SULFUR ABUNDANCE IN THE SLOW SOLAR WIND

C. GIAMMANCO, P. WURZ, AND A. OPITZ

Physikalisches Institut, University of Bern, Bern 3012, Switzerland

AND

F. M. IPAVICH AND J. A. PAQUETTE

Department of Physics and Astronomy and IPST, University of Maryland, College Park, MD 20742, USA

Received 2007 June 29; accepted 2007 September 5

### ABSTRACT

Using 4 years of data from the Mass Time-of-Flight and Proton Monitor, two CELIAS sensors on board *SOHO*, we report the sulfur abundances in comparison to magnesium and calcium (two low first ionization potential elements) for the slow solar wind, and for the first time we measure the sulfur isotopic abundance ratio. For the period in which the proton velocity was  $380 \pm 2 \text{ km s}^{-1}$  we obtain  $[S]/[Mg] = 0.26 \pm 0.03$ ,  $[S]/[Ca] = 4.7 \pm 0.5$ , and  $[^{34}S]/[S] = 0.043 \pm 0.009$ . We compare these measurements with the available measurements reported in the literature, and we check the quality of the results by using the magnesium isotopic ratio and the calcium-to-magnesium abundance ratio as a control. Finally, as a further result we also obtain the absolute abundance of the previous elements. In astronomical notation we have  $A_S = 7.44 \pm 0.04$ ,  $A_{Mg} = 8.03 \pm 0.05$ , and  $A_{Ca} = 6.77 \pm 0.04$ .

*Key words:* solar wind — Sun: abundances — Sun: general

### 1. INTRODUCTION

It is well known that in the corona and solar wind the elements with a low first ionization potential (FIP), below  $\sim 10 \text{ eV}$ , are systematically enriched with respect to their photospheric abundances. This phenomenon is even more evident if we consider the first ionization time (FIT) rather than the FIP, as was shown by Geiss & Bochsler (1986), and in any case the FIP effect is approximately independent of mass. Several models have been proposed to reproduce the observed fractionation pattern. As reported by von Steiger (1996), the general idea of most of them is that the ultraviolet solar photons ionize the atoms and an ion-neutral separation occurs in the lower chromosphere. Marsch et al. (1995) proposed that the separation is realized by the interaction between hydrogen and heavy elements in the presence of a vertical uniform magnetic field. In this first attempt at explanation, they had to invoke possibly somewhat artificial boundary conditions, being different for chromospheric ions and neutrals. More recently, Arge & Mullan (1998) proposed that reconnection events of the magnetic field in the chromosphere heat the ions (but not the neutrals), which would increase the ion density in higher layers. However, this model does not account for the difference between the slow and fast solar wind. Composition measurements of heavy ions in the solar wind show that for the fast solar wind an enrichment of the  $[X]/[O]$  ratio with respect to the photospheric ratio by about a factor of 2 is observed, while for the slow solar wind the enrichment of this ratio is a factor of 4. Then Schwadron et al. (1999) envisaged ion heating by waves coming down from the corona with a wave spectrum specified to give the correct abundance enhancement. Finally, Laming (2004) considered the effect of nonresonant waves on chromospheric ions through the action of the ponderomotive force created by Alfvén waves propagating through the chromosphere. Since the resulting acceleration is independent of the ion mass, in such a model the mass independence of the fractionation comes out naturally, without having to specify a wave spectrum.

In the context of this rich discussion the measurement of sulfur abundance in the solar wind provides an additional constraint. In fact, sulfur is on the border between the low- and high-FIP ele-

ments (FIP = 10.4 eV and FIT = 12 s; Marsch et al. 1995). In recent years the determination of its photospheric abundance has evolved substantially. Recently, Asplund et al. (2005) reported a sulfur photospheric abundance in agreement with the meteoric one. In this paper we present the determination of the elemental ratios  $[S]/[Mg]$  and  $[S]/[Ca]$  in the slow solar wind. Since calcium and magnesium are two low-FIP elements, we will be able to determine the behavior of sulfur in the FIP context comparing the measured ratio value with the corresponding ratios in the photosphere.

Probably the earliest determination of sulfur in the solar wind was made by Shafer et al. (1993), who give a value of  $([S]/[Si])$  for the fast solar wind (in a coronal hole) of  $0.4 \pm 0.15$  and in a driver plasma,  $0.3 \pm 0.12$ . Wurz (1999) found that  $([S]/[O])_{sw}/([S]/[O])_{ph}$  is  $2.3 \pm 0.4$  in the slow solar wind and  $1.4 \pm 0.3$  in the fast solar wind; similar results come from Wurz (2005;  $2.2 \pm 0.8$  and  $1.5 \pm 0.5$ ), supporting the idea that sulfur is between the low- and high-FIP elements. Previous measurements of sulfur in the solar wind were carried out by von Steiger et al. (2000), who report values for the ratio  $[S]/[O]$  for the representative cases of the slow ( $0.050 \pm 0.019$ ) and fast solar wind ( $0.054 \pm 0.014$ ). Finally, in Giammanco et al. (2007) we reported a preliminary analysis of the sulfur abundance, which we improve in the present paper.

### 2. DATA REDUCTION

For our purpose we use 4 years of solar-wind mass spectra provided by the Mass Time-of-Flight (MTOF), one of the CELIAS sensors (Hovestadt et al. 1995) on board *SOHO*. The CELIAS data processing unit accumulates time-of-flight (TOF) spectra every 5 minutes from the ions recorded with the MTOF sensor. The related data are then written in a daily file and marked with the time of acquisition given in international atomic time (TAI). Almost at the same time, the Proton Monitor (PM) sensor, also part of CELIAS, records the velocity, density, and thermal velocity of incoming protons (Ipavich et al. 1998). The information provided by both sensors is suitable to analyze the mass spectra, since the MTOF response (Wurz et al. 1999; Wurz 1999; Giammanco et al. 2007) and the solar-wind characteristics depend on the

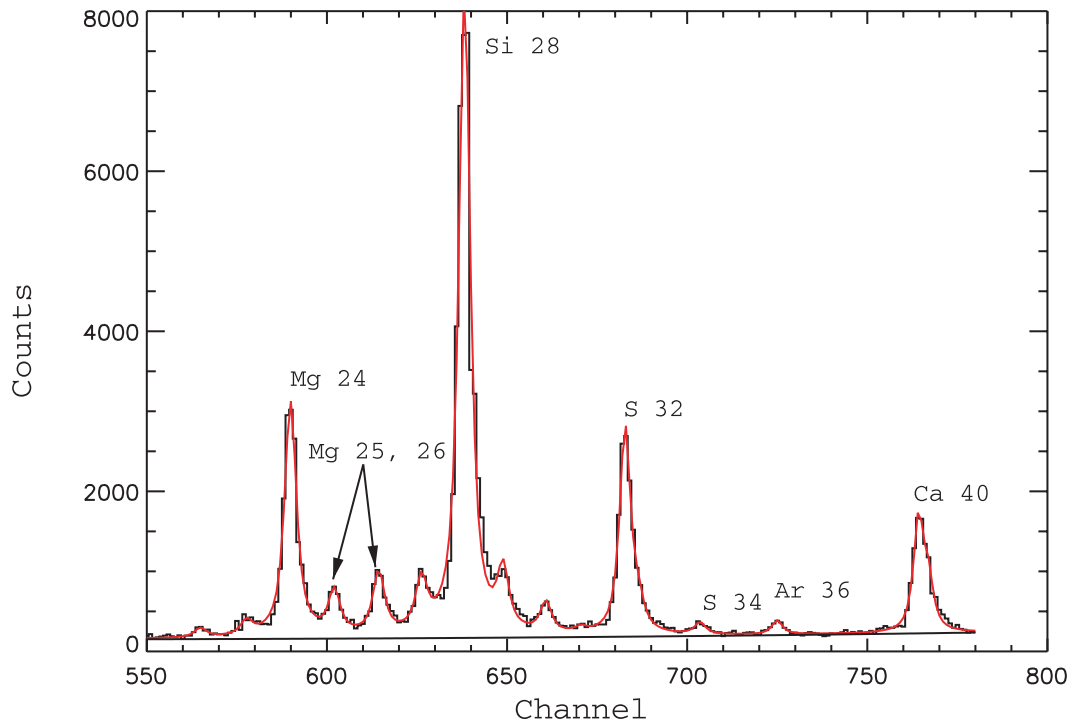


FIG. 1.— Spectrum obtained by summing 851 5 minute spectra, when the proton velocity is in the range  $400 \pm 2 \text{ km s}^{-1}$  and the MTOF sensor voltages are set to  $V_F \sim 10 \text{ V}$  and  $V_{\text{wave}} = 8.774 \text{ kV}$ . The red line shows the fitted curve, and the black line shows the measured histogram. The horizontal black line represents the fitted background.

velocity of incoming protons and heavy ions (Wurz 1999). We select a narrow solar-wind proton velocity interval around  $380\text{--}400 \text{ km s}^{-1}$  with a tolerance of  $\pm 2 \text{ km s}^{-1}$ , in the slow solar-wind range where the PM instrument function is known best. The specific ion velocity is related to the proton velocity via a linear relation (Wurz 1999). Note that the acquisition time of the two sensors can have a delay of some seconds to 1 minute; thus, we interpolate the PM data first to superpose the two temporal axes, then we select only the 5 minute MTOF spectra with the proton speed in the two specified ranges. Once we have the corresponding TAI of the selected data, we check the instrumental status of MTOF, and we integrate all the spectra relative to the same proton speed and instrument status. Then, to have good statistics, we select only the integrated spectra which contain more than 800 5 minute periods.

The status of the MTOF mass spectrometer is determined by two voltages,  $V_{\text{wave}}$  and  $V_F$ , where in general terms  $V_{\text{wave}}$  is responsible for accepting the incoming ions over a large energy per charge range and preventing the solar-wind protons and  $\alpha$ -particles from entering the instrument. The voltage  $V_F$  modifies the total acceptance of the MTOF sensor. The MTOF status and the solar-wind parameter taken by the PM are needed to calculate the MTOF sensor response (Wurz 1999). In addition, the MTOF sensor response is different for every ionization state of an incoming ion. Since MTOF does not measure the charge state, we calculate the charge state distribution using the ionization tables by Mazzotta et al. (1998).

The integrated spectra are from the period between 1996 and 1999, up until the gap in *SOHO* activity. After 1999 the sensitivity of MTOF decreased by a factor of 10. For this reason, also taking into account the years from 1999 to 2006 does not give a significant statistical improvement. On the contrary, recently several problems were identified concerning the determination of the efficiency of *SOHO* after the gap in *SOHO* activity (J. Paquette 2007, private communication). Finally, taking into account 4 years of data ensures a good temporal mean for the values obtained. In

fact, it is known from previous studies that on short timescales there are significant variations in the composition of heavy elements in the solar wind (Wurz 2005).

### 3. RESULTS

For the selected velocity ranges of  $380 \pm 2$  and  $400 \pm 2 \text{ km s}^{-1}$  we have analyzed the spectra obtained for the combination of set voltages  $V_{\text{wave}} = 8744 \text{ V}$  and  $V_F = 10 \text{ V}$ , which are in the interval of a well-determined instrumental response. In order to estimate from these spectra the total number of incoming ions of an element of interest, we fit them by the function

$$f(t) = \sum_i A_i \left\{ \xi \frac{1}{\sqrt{2\pi}\sigma_i} e^{-(t-t_i)^2/2\sigma_i^2} + (1-\xi) \frac{g_i}{\pi[(t-t_i)^2 + g_i^2]} \right\} + c_0 + c_1 t + c_2 t^2 + c_3 t^3,$$

$$\sigma_i = \sigma_{28} \frac{t_{28}}{t_i}, \quad g_i = g_{28} \frac{t_{28}}{t_i},$$

TABLE 1

MEAN COUNTS PER 5 MINUTES IN THE MASS SPECTRA OF THE MTOF SENSOR

Element	$380 \pm 2 \text{ km s}^{-1}$	$400 \pm 2 \text{ km s}^{-1}$
<sup>24</sup> Mg.....	$6.2 \pm 0.3$	$20.8 \pm 0.6$
<sup>25</sup> Mg.....	$1.16 \pm 0.18$	$3.7 \pm 0.3$
<sup>26</sup> Mg.....	$1.74 \pm 0.18$	$5.3 \pm 0.3$
<sup>32</sup> S.....	$10.8 \pm 0.3$	$18.3 \pm 0.9$
<sup>34</sup> S.....	$0.64 \pm 0.12$	$0.91 \pm 0.21$
<sup>40</sup> Ca.....	$8.6 \pm 0.3$	$11.8 \pm 1.5$

NOTE.—The given errors are  $3\sigma$  statistical errors for the fitted parameter of the function in eq. (1).

TABLE 2  
MTOF SENSOR SENSITIVITY DEPENDING ON THE ELEMENT AND ITS CHARGE STATE

Element	VI	VII	VIII	IX	X	XI	XII	XIII	XIV
Proton Speed 380 km s <sup>-1</sup>									
<sup>24</sup> Mg .....	1.51E-03	9.23E-04	4.61E-04	1.83E-04	5.59E-05	1.30E-05	2.36E-06	3.45E-07	4.10E-08
<sup>25</sup> Mg .....	1.63E-03	1.05E-03	5.58E-04	2.42E-04	8.21E-05	2.17E-05	4.47E-06	7.44E-07	1.02E-07
<sup>26</sup> Mg .....	1.74E-03	1.17E-03	6.66E-04	3.12E-04	1.18E-04	3.52E-05	8.27E-06	1.57E-06	2.48E-07
<sup>32</sup> S .....	1.19E-03	1.00E-03	7.65E-04	5.21E-04	3.16E-04	1.68E-04	7.73E-05	3.02E-05	1.01E-05
<sup>34</sup> S .....	1.29E-03	1.13E-03	9.12E-04	6.70E-04	4.46E-04	2.65E-04	1.40E-04	6.48E-05	2.61E-05
<sup>40</sup> Ca .....	2.77E-03	2.61E-03	2.33E-03	1.97E-03	1.56E-03	1.14E-03	7.73E-04	4.83E-04	2.76E-04
Proton Speed 400 km s <sup>-1</sup>									
<sup>24</sup> Mg .....	2.59E-03	1.86E-03	1.15E-03	6.03E-04	2.63E-04	9.29E-05	2.64E-05	6.09E-06	1.17E-06
<sup>25</sup> Mg .....	2.71E-03	2.02E-03	1.31E-03	7.27E-04	3.42E-04	1.33E-04	4.21E-05	1.09E-05	2.35E-06
<sup>26</sup> Mg .....	2.80E-03	2.16E-03	1.47E-03	8.63E-04	4.37E-04	1.86E-04	6.54E-05	1.90E-05	4.61E-06
<sup>32</sup> S .....	1.84E-03	1.64E-03	1.37E-03	1.06E-03	7.48E-04	4.80E-04	2.77E-04	1.43E-04	6.53E-05
<sup>34</sup> S .....	1.89E-03	1.74E-03	1.51E-03	1.23E-03	9.33E-04	6.49E-04	4.14E-04	2.41E-04	1.26E-04
<sup>40</sup> Ca .....	3.61E-03	3.50E-03	3.27E-03	2.92E-03	2.50E-03	2.03E-03	1.55E-03	1.11E-03	7.48E-04

where the index  $i$  is the mass number of the element and the variable  $t$  is the channel number in the TOF spectrum of the recorded atoms. In equation (1) the peaks for each element are described by a combination of a Gaussian and Lorentzian function, and the background is described by a third-order polynomial. The peak widths  $\sigma_i$  and  $g_i$  are scaled proportional to their TOF. As we show in Figure 1 the fit agrees with the measured data very well and does not present a limitation to further analysis. In Table 1 we report the mean counts per 5 minutes found for each analyzed element.

In order to compare the counts obtained for two different elements, we have to divide them by the instrument function. As discussed in the previous section this function also depends on the ionization state of the incoming atoms. In Table 2 we give the instrument function for the various charge states of the ions of interest. Since we do not perform simultaneous measurement of the ionization state, we use the Mazzotta et al. (1998) tables and model the freeze-in temperature depending on the wind velocity (Wurz 1999). The final results are shown in Table 3, where we

also give the estimated abundance of the analyzed elements relative to hydrogen. The latter is possible thanks to the proton density measurements carried out by the PM.

#### 4. DISCUSSION AND CONCLUSIONS

In this paper we present the measurement of the element ratio of sulfur compared to calcium and magnesium in the regime of the slow solar wind. We measure the peaks of the three elements from the same spectrum using only one fit function (which supposes the same shape for all peaks in the range; eq. [1]). As an additional test of the quality of the measurement, we also present the ratio of Mg and Ca in Table 3. Both Mg and Ca are low-FIP elements, and according to the general understanding of the FIP fractionation process, they must follow the same fractionation, maintaining a constant ratio from the photosphere to the solar wind and meteoric values. As a second test we check the isotopic abundance of <sup>34</sup>S, which at the same time represents the first measurement of this isotope. In the solar wind the results agree well

TABLE 3  
RESULTS OF ABUNDANCE DETERMINATION USING THE MTOF SENSOR

ABUNDANCE	PRESENT MEASUREMENTS		LITERATURE DATA			
	380 ± 2 km s <sup>-1</sup>	400 ± 2 km s <sup>-1</sup>	Solar Wind	Photosphere <sup>a</sup>	Meteorites <sup>b</sup>	Earth <sup>c</sup>
[S]/[Mg].....	0.26 ± 0.03	0.25 ± 0.03	0.34 ± 0.15 <sup>d</sup>	0.41 ± 0.06	0.43 ± 0.06	...
[S]/[Ca].....	4.7 ± 0.5	4.3 ± 0.8	...	6.8 ± 0.6	7.4 ± 1.2	...
[ <sup>34</sup> S]/[S].....	0.043 ± 0.009	0.04 ± 0.01	...	...	...	0.043 ± 0.003
[ <sup>25</sup> Mg]/[ <sup>24</sup> Mg] .....	0.13 ± 0.02	0.14 ± 0.01	0.130 ± 0.007, <sup>e</sup> 0.130 ± 0.007 <sup>f</sup>	...	...	0.1266 ± 0.0001
[ <sup>26</sup> Mg]/[ <sup>24</sup> Mg] .....	0.146 ± 0.017	0.16 ± 0.01	0.138 ± 0.012, <sup>f</sup> 0.14 ± 0.01 <sup>e</sup>	...	...	0.1394 ± 0.0001
[Mg]/[Ca] .....	18.0 ± 1.8	17.6 ± 2.9	...	16.5 ± 1.2	17 ± 2	...
$A_S$ .....	7.44 ± 0.04	7.35 ± 0.05	...	7.14 ± 0.05	7.19 ± 0.04	...
$A_{Mg}$ .....	8.03 ± 0.05	7.96 ± 0.04	...	7.53 ± 0.09	7.56 ± 0.02	...
$A_{Ca}$ .....	6.77 ± 0.04	6.71 ± 0.08	6.63 ± 0.05 <sup>g</sup>	6.31 ± 0.04	6.32 ± 0.03	...

NOTES.—Here  $A_X$  refers to the astronomical abundance relative to hydrogen,  $A_X = \log n_X/n_H + 12$ , Mg refers to the sum of all isotopic abundances, and S refers to <sup>32</sup>S + <sup>34</sup>S. The errors we give for our measurements are 3  $\sigma$  values, considering the statistical uncertainty, curve-fitting, and uncertainty in the instrument function. The errors of our abundance data ( $A_X$  values) are 1  $\sigma$ , as are the errors for the literature data.

<sup>a</sup> Asplund et al. (2005).

<sup>b</sup> Recompilation of CI chondrites by Lodders (2003).

<sup>c</sup> Rosman & Taylor (1998).

<sup>d</sup> From von Steiger et al. (2000). The value is representative of the slow solar wind.

<sup>e</sup> From Wimmer-Schweingruber et al. (1999). The value is representative of the slow solar wind.

<sup>f</sup> From Kucharek et al. (1998). The value is representative of the slow solar wind in 1996.

<sup>g</sup> From Wurz et al. (2003). The value is representative of the slow solar wind.

with the values observed in meteorites and on Earth. Finally, observing the abundance of sulfur relative to calcium and magnesium taken from Table 3, we find that in both cases the measured ratio is two-thirds of the meteoric one. For both velocity ranges we obtain

$$\left(\frac{[\text{S}]}{[\text{Mg}]}\right)_{\text{sw}} \left(\frac{[\text{Mg}]}{[\text{S}]}\right)_{\text{met}} = 0.60 \pm 0.15,$$

$$\left(\frac{[\text{S}]}{[\text{Ca}]}\right)_{\text{sw}} \left(\frac{[\text{Ca}]}{[\text{S}]}\right)_{\text{met}} = 0.64 \pm 0.14.$$

This comparison also supports the concept that sulfur is a border element between the low- and high-FIP elements, since its enrichment in the slow solar wind is less than that of a typical low-FIP element like magnesium or calcium. Laming (2004) modeled the FIP fractionations of the different elements as a function of the Alfvén wave energy density and found good correspondence

between the model values and observational values (Feldman & Laming 2000; Feldman & Widing 2003) at an energy density of  $0.04 \text{ ergs cm}^{-3}$ . In agreement, our sulfur fractionation measurement ( $1.6 \pm 0.4$ ) points to an energy density between 0.028 and  $0.04 \text{ ergs cm}^{-3}$ .

Unfortunately, the same analysis for the fast solar wind could not be performed with the same quality, which is why the results are not shown here. However, it is expected that the fractionation is less in the fast solar wind. The earlier results from Shafer et al. (1993) and Wurz (1999, 2005) support this picture. Only the results from von Steiger et al. (2000) appear to show a different behavior, i.e., that sulfur behaves like a high-FIP element, where the S/O ratio is the same for the slow and fast solar wind.

We gratefully acknowledge the referee, J. Martin Laming, for the useful comments that helped to enrich this paper, and the Swiss National Foundation for continuous financial support.

#### REFERENCES

- Arge, C. N., & Mullan, D. J. 1998, *Sol. Phys.*, 182, 293  
 Asplund, M., Grevesse, N., & Sauval, J. 2005, in *ASP Conf. Ser.* 336, *Cosmic Abundances as Records of Stellar Evolution and Nucleosynthesis*, ed. T. G. Barnes III & F. N. Bash (San Francisco: ASP), 25  
 Feldman, U., & Laming, J. M. 2000, *Phys. Scr.*, 61, 222  
 Feldman, U., & Widing, K. G. 2003, *Space Sci. Rev.*, 107, 665  
 Geiss, J., & Bochsler, P. 1986, in *The Sun and the Heliosphere in Three Dimensions*, ed. R. G. Marsden (Dordrecht: Reidel), 173  
 Giammanco, C., Bochsler, P., Karrer, R., Ipavich, F., Paquette, J., & Wurz, P. 2007, *Space Sci. Rev.*, 130, 329  
 Hovestadt, D., et al. 1995, *Sol. Phys.*, 162, 441  
 Ipavich, F. M., et al. 1998, *J. Geophys. Res.*, 103, 17205  
 Kucharek, H., et al. 1998, *J. Geophys. Res.*, 103, 26805  
 Laming, J. M. 2004, *ApJ*, 614, 1063  
 Lodders, K. 2003, *ApJ*, 591, 1220  
 Marsch, E., von Steiger, R., & Bochsler, P. 1995, *A&A*, 301, 261  
 Mazzotta, P., Mazzitelli, G., Colafrancesco, S., & Vittorio, N. 1998, *A&AS*, 133, 403  
 Rosman, K. J. R., & Taylor, P. D. P. 1998, *Pure Appl. Chem.*, 70, 217  
 Schwadron, N. A., Fisk, L. A., & Zurbuchen, T. H. 1999, *ApJ*, 521, 859  
 Shafer, C. M., Gloeckler, G., Galvin, A. B., Ipavich, F. M., Geiss, J., von Steiger, R., & Ogilvie, K. 1993, *Adv. Space Res.*, 13, 79  
 von Steiger, R. 1996, in *AIP Conf. Proc.* 382, *Solar Wind Eight*, ed. D. Winterhalter et al. (New York: AIP), 193  
 von Steiger, R., et al. 2000, *J. Geophys. Res.*, 105, 27217  
 Wimmer-Schweingruber, R. F., Bochsler, P., & Wurz, P. 1999, in *AIP Conf. Proc.* 471, *Solar Wind Nine*, ed. S. R. Habbal et al. (New York: AIP), 147  
 Wurz, P. 1999, Habilitation thesis, Univ. Bern  
 ———. 2005, in *The Dynamic Sun: Challenges for Theory and Observations*, ed. D. Danesy et al. (ESA SP-600; Noordwijk: ESA), 44  
 Wurz, P., Bochsler, P., Paquette, J. A., & Ipavich, F. M. 2003, *ApJ*, 583, 489  
 Wurz, P., et al. 1999, *Phys. Chem. Earth C*, 24, 421